Proceedings of
The Fourth National Congress on Fluids Engineering
August 23-25, 2006, Kyungju, Korea

Ballistic Range Simulator 의 최적화에 관한 수치계산 및 이론해석적 연구

Rupal Mishra* · 강현구** · G. Rajesh*** · 이정민**** · 김희동*****

Computational and Theoretical Studies on the Optimization of A Ballistic Range Simulator

Rupal Mishra*, H. G. Kang**, G. Rajesh***, J. M. Lee****, H. D. Kim*****

Keywords : Ballistic Range(발리스틱 레인지), Shock Tube(충격파관), Ballistic Efficiency(발리스틱 효율), Unsteady Flow(비정상 유동), Projectile(발사체)

1. Introduction

The ballistic range is a fluid dynamic device that can accelerate a projectile to high supersonic or hypersonic speeds through a shock compression. Recently much interest has been concentrated on creating an extremely high-pressure state over several tens to hundreds thousand atmosphere and thereby achieving very high enthalpy flows using ballistic range [1, 2].

In general, the ballistic range consists of three tubes, two diaphragms, a piston and a projectile as schematically shown in Fig. 1. A high-pressurized tube serves as the reservoir of high-pressure gas. Usually this high-pressure is created by firing an explosive in the high-pressure tube. A pump tube which contains a light gas is connected to the high-pressure tube through a diaphragm separating both at the junction. A massive piston is placed very near to the diaphragm in the pump tube. Projectile is placed in the launch tube which is connected to the pump tube through another diaphragm. Rupture of the diaphragm between the high-pressure tube and pump tube causes the piston to move at a high-speed and isentropically compress the light-gas to a much higher pressure than that in the high-pressure tube, and the second diaphragm is ruptured initiating a high-speed flow with the production of a strong unsteady shock wave in the launch tube. Resulting high-pressure state behind the projectile produced by the reflection of the shock wave on the projectile base, drives the projectile with a very high-velocity.

Until now, a large number of pioneering works [3-4] have been carried out to optimize the performance of the ballistic range simulators and to effectively design the device. It has been known [3, 4] that the best performance of the ballistic range would be obtained when the projectile base pressure could be kept constant.

* Summer Intern Student, Andong National University
** Graduate Student, Andong National University
*** Doctoral Student, Andong National University
**** Director, Angang Plant, Pungsan Co.
***** Professor, School of Mechanical Engineering, Andong National University, E-mail: kimhd@andong.ac.kr
TEL: (054) 820-5622, FAX: (054) 820-6127

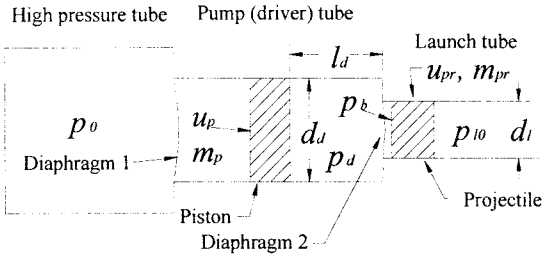

Fig. 1 Schematic of Ballistic Range

A lot of other theoretical and experimental works [5-8] were devoted to the performance improvement of various types of ballistic ranges. Bogdanoff & Miller [5] investigated the effect of adding a diaphragm in the pump tube on the performance of ballistic range. According to their results, the performance of the ballistic range is improved with the addition of the diaphragm due to the reduction of maximum pressure in the device. Since the addition of a shock tube can give some advantage over the conventional ballistic range, as it can control the shock strength, and/or mount the projectile in the launch tube, the various processes involved need to be analyzed carefully to optimize the performance of the device.

The objective of the present study is to analyze the performance of ballistic range employed to investigate aerodynamics and aeroballistics in the hyper-velocity regime. The effect of adding shock tube in between the pump tube and the launch tube has also been analyzed. The present analysis helps to identify the range of operating parameters in which the device shows a significant performance enhancement with and without the shock tube.

2. Analytical Study

2.1 Methodology

The schematic diagram of a typical ballistic range is shown in Fig. 1. The motion of the piston in the pump tube is implicitly decided by the difference of pressures on both sides of it. It is assumed that the high-pressure tube can supply high-pressure gas at constant rate. While modeling the motion of the piston, driver gas inertia is neglected with

dissipation effects caused by the flow and friction between the piston and the pump tube wall.

The projectile is driven by the unsteady shock wave in the launch tube. The pressure acting on the base of the projectile can be found using the unsteady gas dynamic equations, with the assumption that no reflected rarefaction wave from the piston overtakes the projectile.

2.2 Piston Motion

The piston is assumed to be accelerating from an initial state where the pressure is equal to that in the high-pressure tube and the velocity is zero.

Using method of characteristics, the pressure acting on the rear side of the piston at any time is given as,

$$p = p_0\left\{1-\frac{u_p}{a_0}\left(\frac{\gamma_0-1}{2}\right)\right\}^{\frac{2\gamma_0}{\gamma_0-1}} \tag{1}$$

On the front side of piston, the driver gas is being compressed isentropically. Using isentropic relations,

$$\frac{p_d}{p_{d_0}}=\left(\frac{x_d}{l_d}\right)^{-\gamma_d}=\lambda^{-\gamma_d}, \text{ where, } \lambda \text{ is the compression ratio} \tag{2}$$

Equation of motion of the piston reduces to

$$-m_p\left(\frac{d^2x_d}{dt_p^{\,2}}\right)=\frac{\pi.d_d^{\,2}}{4}\left[p_{d_0}\lambda^{-\gamma_d}-p_0\left\{1-\frac{u_p}{a_0}\left(\frac{\gamma_0-1}{2}\right)\right\}^{\frac{2\gamma_0}{\gamma_0-1}}\right] \tag{3}$$

With the use of dimensionless variables,

$$\xi(\tau)=\frac{x_d}{d_d},\quad \tau=\frac{t_p.a_0}{d_d},\quad \phi(\tau)=\frac{u_p}{a_0} \tag{4}$$

Eq. (3) can be written as,

$$\dot{\xi}=-\phi,\ \dot{\phi}=-c_1\left\{c_2\xi^{-\gamma_d}-\left(1-\frac{\gamma_0-1}{2}\right)^{\frac{2\gamma_0}{\gamma_0-1}}\right\} \tag{5}$$

$$\xi(0)=\frac{l_d}{d_d},\quad \phi(0)=0$$

where, c_1 and c_2 are given by

$$c_1=\frac{\pi}{4}\frac{p_0.d_d^{\,3}}{m_p.a_0^{\,2}},\ c_2=\frac{p_{d_0}}{p_0}\left(\frac{l_d}{d_d}\right)^{\gamma_d} \tag{6}$$

Eq. (5) is solved using Runge-Kutta method.

2.2 Projectile Motion

Equation of motion of projectile is modeled with the use of unsteady shock wave generated due to diaphragm rupture, and is given by

$$m_{pr}\frac{d^2x_l}{dt_{pr}^{\,2}}=\frac{\pi d_l^{\,2}}{4}\left(p_b-p_{l_0}\right) \tag{7}$$

where, p_b is the shock compression pressure on the base of the projectile. For a tube with cross-sectional area change, the pressure due to diaphragm rupture is given by [6],

$$\frac{p_b}{p_r}=g\left\{1-g^{-\left(\frac{\gamma_d-1}{2\gamma_d}\right)}\frac{\gamma_d-1}{2}\left(\frac{u_{pr}}{a_r}\right)\right\}^{\frac{2\gamma_d}{\gamma_d-1}} \tag{8}$$

where, g is the equivalence factor based on area reduction and is given by,

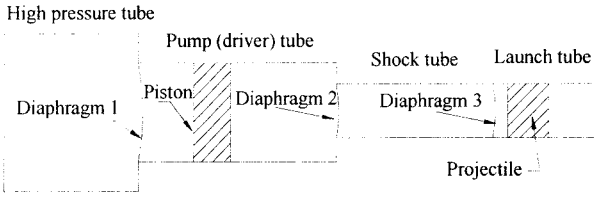

Fig. 2 Schematic of ballistic range with shock Tube

$$g=\left[\frac{(\gamma_d+1)\{2+(\gamma_d-1)M_e^{\,2}\}}{\{2+(\gamma_d-1)M_e\}^2}\right]^{\frac{\gamma_d}{\gamma_d-1}} \tag{9}$$

Assuming choked flow immediately after the diaphragm rupture, *Me* can be found out form Mach number-Area ratio relation.

With the use of dimensionless parameters,

$$\chi=\frac{\pi d_l^{\,2}}{4}\frac{p_r}{m_{pr}a_r^{\,2}}x_l,\ \zeta=\frac{\pi d_l^{\,2}}{4}\frac{p_r}{m_{pr}a_r}t_{pr},\ \psi=\frac{u_{pr}}{a_r}, \tag{10}$$

Eq. (7) with the initial conditions becomes

$$\frac{d^2\chi}{d\zeta^2}=g\left[1-g^{-\left(\frac{\gamma_d-1}{2\gamma_d}\right)}\frac{\gamma_d-1}{2}\psi\right]^{\frac{2\gamma_d}{\gamma_d-1}}-\frac{1}{DPR}$$

$$\chi(0)=0,\qquad \dot{\chi}(0)=0 \tag{11}$$

where, p_r, and a_r are the pressure and the speed of sound at diaphragm rupture, respectively, and *DPR* is the diaphragm pressure ratio, defined as p_r/p_{l0}.

2.2 Addition of Shock tube

The schematic of ballistic range with a shock tube is shown in Fig. 2. Projectile is accelerated in launch tube due to the double compression of gases using piston motion and unsteady shock wave.

Pressure ratio across the normal shock wave traveling into the shock tube can be written as,

$$\frac{p_{s_0}}{p_{r_d}}=\frac{1}{\Pi_{21}}\left[1-(\Pi_{21}-1)\left(\frac{(\gamma_d-1)}{2\gamma_d}\left(\frac{K\frac{T_{s_0}}{T_{r_s}}}{\frac{\gamma_s+1}{\gamma_s-1}\Pi_{21}+1}\right)\right)^{\frac{1}{2}}\right]^{\frac{2\gamma_d}{\gamma_d-1}} \tag{12}$$

where, $\Pi_{21}=p_2/p_1$ is the pressure ratio across the shock wave, and p_{s0}/p_{rd} is the pressure ratio across the pump tube diaphragm. *K* is the ratio of specific heats of pump tube and shock tube gases at constant volume. From the normal shock relations, the pressure ratio across the reflected shock wave is obtained as,

$$\Pi_{ref}=\frac{p_{ref}}{p_2}=\frac{\frac{\gamma_s+1}{\gamma_s-1}+2-\Pi_{21}}{1+\frac{\gamma_s+1}{\gamma_s-1}\Pi_{21}} \tag{13}$$

3. Computational Study

The computational study is performed by a commercial software CFD-FASTRAN. It is a density based finite volume computational fluid dynamics code which solves the two-dimensional Euler equations. The Solver uses point Jacobi implicit scheme with backward Euler descretization

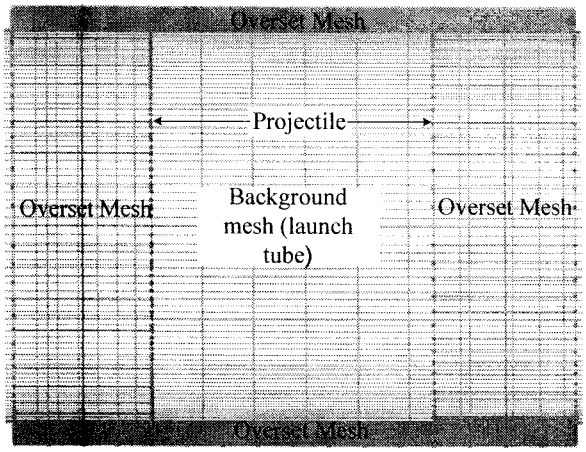

Fig. 3 Chimera (overset) mesh system on projectile

of the domain. The spatial differencing scheme is Rhoe's approximated Riemann solver. The flow is considered unsteady and inviscid.

For simulating the motion of the projectile and piston, chimera mesh technology is used. Overset meshes are constructed along the 4 sides of the projectile, as shown in Fig. 3, to interpolate the data from the other zones on which the meshes are overlapped, while the former is in motion. Projectile is identified as the moving body and is modeled with 6 degree of freedom motion requiring inputs as projectile mass, 3 moments of inertia and Y, Z co-ordinate constraints.

4. Performance Optimization

Only a few works have been made to assess the efficiency of a ballistic range to date. According to these results, the ballistic efficiency is defined as the ratio of the rate of change of kinetic energy of the projectile to the rate of expenditure of gas energy [8]. From a practical design point of view of the ballistic range, the endurance limit of the projectile at very high pressures can be of major concern. In this context, the piezometric ratio is defined as the ratio of the peak pressure to the average pressure at the base of the projectile during its flight [8].

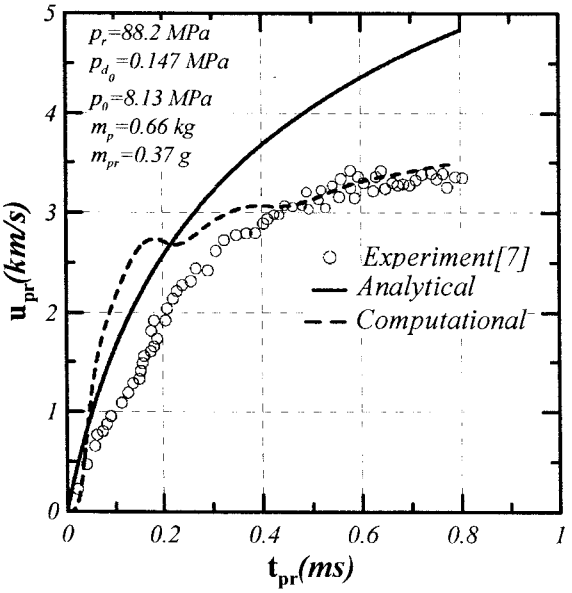

Fig. 4 Comparison of projectile velocities

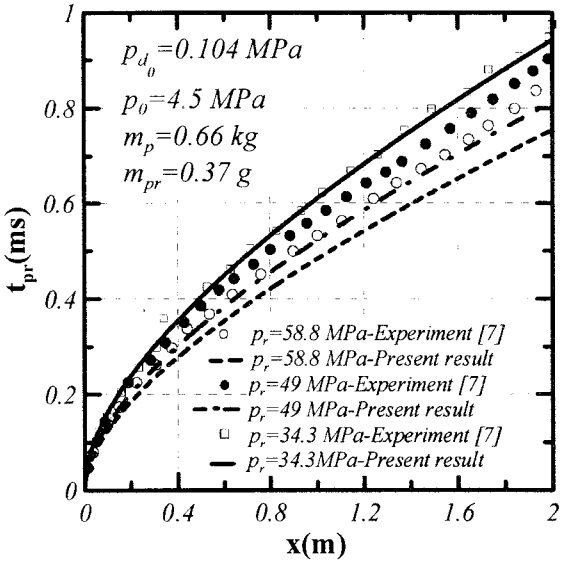

Fig. 5 Comparison of projectile paths

In the present study, it is assumed that the gas pressure in the high-pressure tube is kept constant during the complete operation of the ballistic range and when the energy of the high-pressure gas is being transferred to the projectile, there may be losses in both high-pressure tube and pump tube. These losses can be excluded if the compression work done by the piston and the energy of the pump tube gas at the time of diaphragm rupture are considered to assess the performance of the ballistic range.

The time at which the projectile reaches constant velocity is considered to obtain average kinetic energy of the projectile. The ballistic efficiencies based on the isentropic work done by the piston and gas energy at the time of rupture can thus be expressed as

$$\eta_p = \frac{\frac{1}{t_{pr}}\int_0^{t_{pr}}\left(0.5u_{pr}^2\right)dt_{pr}}{\frac{a_d\left(\frac{T_r}{T}-1\right)}{\gamma_d(\gamma_d-1)}}, \quad \eta_g = \frac{\frac{1}{t_{pr}}\int_0^{t_{pr}}\left(0.5u_{pr}^2\right)dt_{pr}}{\frac{p_r}{\rho_r}} \tag{14}$$

For the same time period for which the projectile velocity becomes constant, the piezometric ratio can be written as,

$$\eta_{piezo} = \frac{p_{b\max}}{\frac{1}{t_{pr}}\int_0^{t_{pr}} p_b dt_{pr}} \tag{15}$$

5. Results and discussion

5.1 Validation of the present analysis

In Fig. 4, the present analytical and computational results are validated with the experimental ones [7]. The theoretical and computational projectile velocities are over-predicted due to the assumption of non-isentropic conditions. The difference between computational and analytical results is due to the poor simulation resulted from the chimera mesh and boundary conditions. However the general agreement is good. In Fig. 5, the predicted projectile path is compared with experimental results [7] for various diaphragm rupture pressures. At low diaphragm

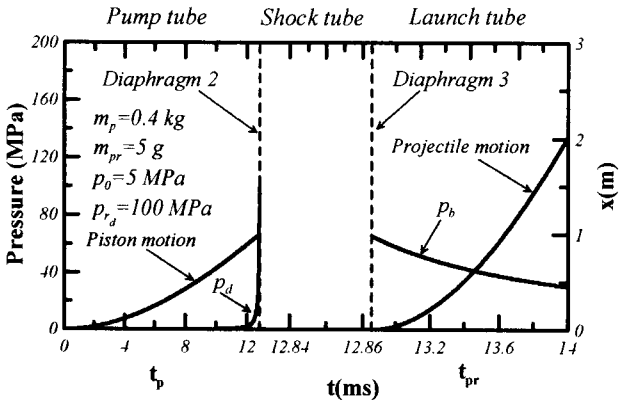

Fig. 6 Operating processes of ballistic range with shock tube

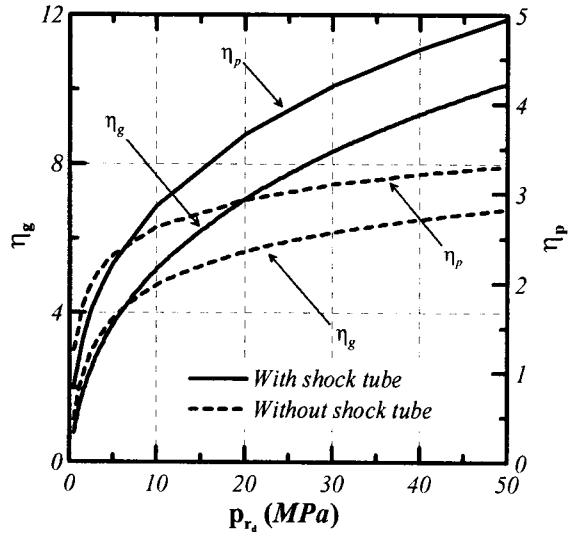

Fig.7 Variation of ballistic efficiencies

rupture pressures, the agreement between the analysis and experiment is excellent. However, as the diaphragm rupture pressure increases, the agreement becomes poor due to the non-isentropic conditions arising at higher diaphragm rupture pressures, and the wave and friction drags at higher velocities.

Fig. 6 shows the typical operating processes of ballistic range with shock tube. Figs.7 and 8 shows the variation of ballistic efficiencies η_p and η_g , η_{piezo} and projectile velocity with respect to the pump tube diaphragm rupture pressure, p_{rd}. It is known that for both the ballistic ranges with and without shock tube, η_p, η_g, η_{piezo} and projectile

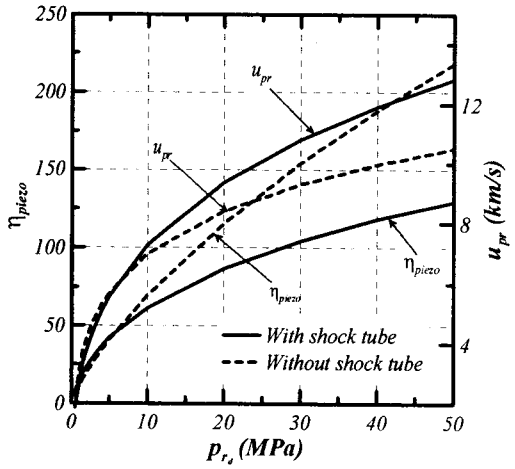

Fig. 8 Variation of piezometric ratio and velocity

velocity increase with p_{rd}. At large values of rupture pressure, the ballistic range with shock tube shows significant performance improvement. However, the ballistic range without shock tube performs slightly better than the other at very low rupture pressures. This identifies the ranges under which both the ballistic ranges can be operated at its maximum performance.

The analysis reveals that significant performance enhancement could be obtained with the addition of a shock tube. However, the present analysis being unable to model various dissipation effects, the calculated performance enhancement with the addition of shock tube in the ballistic range may be over-estimated.

6. Conclusions

Both theoretical and computational analyses have been carried out to identify the range of parameters under which the ballistic range performance becomes maximum. Ballistic efficiencies defined here, clearly dictate how efficient the energy transfer is from the pump tube to the projectile. Lower piezometric ratios correspond to even distribution of the shock pressure on the projectile during its flight.

A considerable improvement of ballistic range performance was obtained with the addition of a shock tube. The analysis reveals that the shock tube added to ballistic range improves the performance of the device at higher diaphragm rupture pressures. Best operating conditions of the device could thus be identified from the present investigation. Further analysis needs to be carried out for simulating the viscous conditions in the ballistic range.

References

[1] Chhabildas, L. C., Kmetyk, L. N., Reinhart, W. D. and Hall, C. A., 1995, "Enhanced Hypervelocity Launcher – Capabilities to 16 Km/s," Intl. J. Impact Engineering., Vol. 17.

[2] Timothy, G. T. and Lalit, C. C., 1995, "Computational Design of Hypervelocity Launchers," Intl. J. Impact Engineering, Vol. 17.

[3] Smith, F., 1963, "Theory of Two Stage Hypervelocity Launcher to Give Constant Driving Pressure at the Model," J. Fluid Mechanics, Vol. 17.

[4] Lukasiewics, J., 1967, "Constant Acceleration Flows and Applications to High Speed Guns," J. AIAA, Vol. 5, No. 11.

[5] Bogdanoff, D. W. and Miller, R. J., 1995 "Improving the Performance of Two Stage Light Gas Guns by Adding a Diaphragm in the Pump Tube," Intl. J. Impact Engineering, Vol. 17.

[6] Glass, I. I. and Sislian, J. P., 1994, "Nonstationary Flows and Shock Waves," Oxford Science Publications, Oxford, pp. 100-125.

[7] Goro, K., Akimasa, T. and Kaoru, O., 1974, "Studies of Hyper-velocity Model Launcher," J. The Japan Society for Aeronautical and Space Sciences, Vol. 22, No. 24.

[8] Horst, A., Baker, P., Rice, B., Kaste, P., Colburn, J. and Hare, J., 2001, "Insensitive High Energy Propellants for Advanced Gun Concepts," Proc. 19th Intl. Symposium of Ballistics, Switzerland.